Directed Enzymatic Activation of 1-D DNA Tiles

Sudhanshu Garg,[*,†] Harish Chandran,[†,‡] Nikhil Gopalkrishnan,[†,§] Thomas H. LaBean,[†,⊥] and John Reif[*,†]

[†]Department of Computer Science, Duke University, Durham, North Carolina 27708, United States, [‡]Google, Mountain View, California 94043, United States, [§]Wyss Institute for Biologically Inspired Engineering, Harvard University, Boston, Massachusetts 02115, United States, and [⊥]Department of Materials Science and Engineering, North Carolina State University, Raleigh, North Carolina 27606, United States

ABSTRACT The tile assembly model is a Turing universal model of self-assembly where a set of square shaped tiles with programmable sticky sides undergo coordinated self-assembly to form arbitrary shapes, thereby computing arbitrary functions. Activatable tiles are a theoretical extension to the Tile assembly model that enhances its robustness by protecting the sticky sides of tiles until a tile is partially incorporated into a growing assembly. In this article, we experimentally demonstrate a simplified version of the Activatable tile assembly model. In particular, we demonstrate the simultaneous assembly of protected DNA tiles where a set of inert tiles are activated *via* a DNA polymerase to undergo linear assembly. We then demonstrate stepwise activated assembly where a set of inert tiles are activated sequentially one after another as a result of attachment to a growing 1-D assembly. We hope that these results will pave the way for more sophisticated demonstrations of activated assemblies.

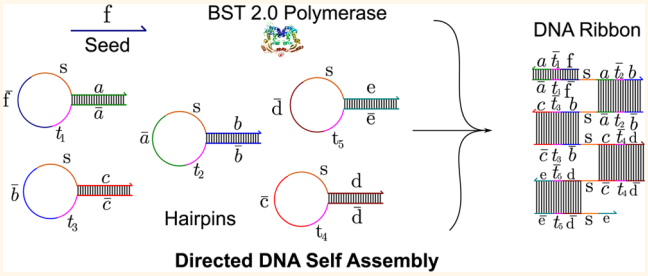

KEYWORDS: DNA self assembly · DNA Polymerase · DNA tile · directed assembly · sequential assembly

DNA Self-Assembly. DNA nanotechnology is a rapidly emerging discipline that uses the molecular recognition properties of DNA to create artificial structures out of DNA. Precise nanoscale objects can be programmatically created using self-assembly of DNA strands, and this has resulted in a myriad of nanostructures.[1−10] But more importantly, the dynamic behavior of these DNA nanostructures can also be controlled *via* the action of other DNA strands[11−17] and enzymes that act on the DNA strands.[18−20]

An important class of DNA nanostructures are tile-based assemblies which are formed *via* addition of DNA tiles to a growing lattice. The tiles have sticky ends known as pads, which are ssDNA that allow the tile to bind specifically to other tiles having the complementary pads (complementary ssDNA). Winfree *et al.*[1] demonstrated the first lattices self-assembled from DNA tiles. Since then, many DNA lattices, 2D and 3D, have been demonstrated.[3,5,10] When the sticky ends of various tiles are carefully programmed, complex lattices can be created.[21,22] Rothemund and Winfree[23] showed in theory that any computable function can be implemented *via* a set of tiles with carefully designed sticky ends.

Computational Power of 1-D Tile Assembly. Adleman first demonstrated that 1-D self-assembly can be used to solve an instance of an intractable problem.[24] Winfree *et al.*[25] proved that linear assembly was equivalent to regular languages and, hence, were as powerful as a finite state automaton. Reif[26,27] proposed simple linear tiling self-assemblies for operations such as integer addition, prefix XOR summing of *n* Boolean bits, string fingerprinting and finite state automata simulations. These were the basis of DNA tiling experiments of Mao *et al.*[28] These linear tilings were refined by Winfree *et al.*[29] to a class of String Tilings. LaBean *et al.* used these tilings to synthesize a full-adder by using two distinct sets of sticky-ends between adjacent tiles in the assembly to effectively communicate the values of the carry-bits.[30] Linear assemblies have also been a subject of study in theoretical self-assembly.[31] They can be used for making frame tiles,[26] as boundaries,[32] and for arranging nanodots/bioagents in a particular pattern.[33]

* Address correspondence to sgarg@cs.duke.edu, reif@cs.duke.edu.

Received for review August 14, 2014 and accepted January 27, 2015.

Published online January 27, 2015
10.1021/nn504556v

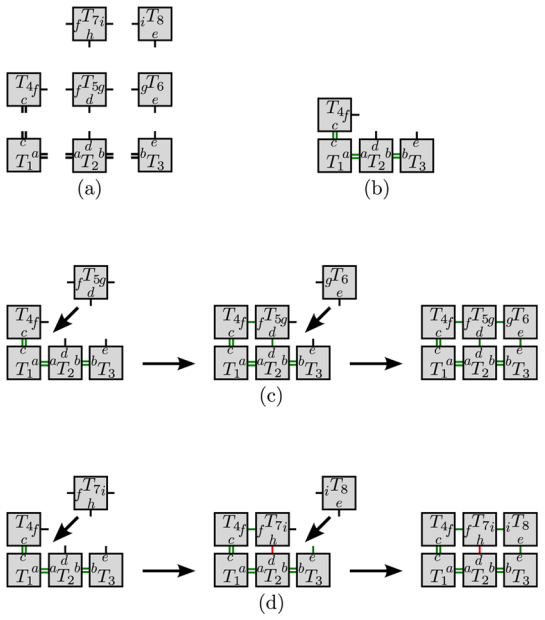

Figure 1. Mechanism of cooperative growth errors. (a) An 8 tile system with a potential for cooperative binding errors in the tile assembly model.[42] Tiles are represented by gray rectangles with face labels. Pad types are shown near the appropriate edge of each tile. Null pads are omitted. Pad strength is indicated by the number of rectangular bars that accompany each pad. Tile system is run at temperature $\tau = 2$. (b) Initial error free assembly of 4 tiles. Correctly matched pads are shaded green. (c) Error free assembly pathway to completion from state (b). (d) Erroneous pathway due to cooperative binding error. Mismatched pad highlighted in red.

Errors in Tile Assembly. Experimental demonstration of complex tilings have been limited by significant assembly errors. Errors in experimental self-assembly have ranged in 1-D from 2 to 5%,[28] and in 2-D from 10% in 2004,[22] 1.7% in 2007,[34] 0.13% in 2009,[35] 0.05% in 2010,[36] to 0.02% in replicating bits of information.[37]

Theoretical solutions have been suggested to remedy growth errors, facet errors and nucleation errors that arise in DNA tilings.[38−40] A major source of errors are *cooperative growth errors*, which occur when a tile's sticky ends match with only some of its neighbors but that is sufficient for it to be wrongly incorporated into the assembly. If we make sure that cooperative growth errors (Figure 1) are fixed, a 6-fold increase in error-free assemblies is theoretically possible.[41] Though the trends show a marked decrease in per step assembly errors, final compounded error rates for the global assembly are still high enough to make large-scale defect free assemblies infeasible at the moment.

Majumder and Reif[43] described a novel protection/deprotection strategy to strictly enforce the direction of tiling assembly growth to ensure the robustness of the assembly process. In their system, tiles are initially inactive, meaning that each tile's output sticky ends are protected and cannot bind with other tiles. Only after other tiles bind to the tile's input sticky ends does the tile transition to an active state and its output sticky

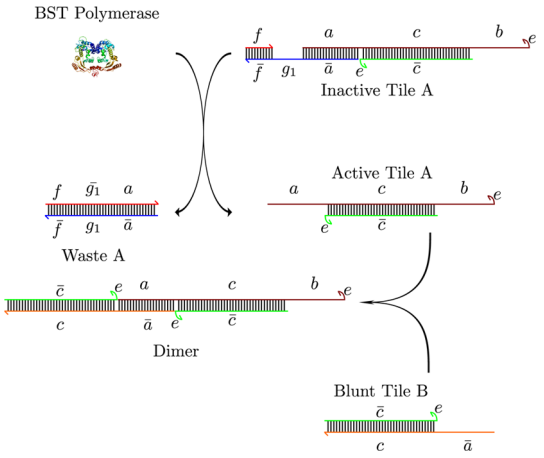

Figure 2. Dimerization of *Tile A* and *Tile B* after activation: *Inactive Tile A* is transformed into *Active Tile A* by the strand displacing *BST DNA Polymerase*. *Blunt Tile B* is a modified version of *Active Tile B* that lacks the sticky end $\bar{b}$. This prevents the formation of a linear polymer and assembly is halted after a dimer (*Active Tile A* and *Blunt Tile B*) is produced.

ends are exposed, allowing further growth, and the formation of an assembly. In this paper, we demonstrate a 1-D activatable assembly. Though 1-D assemblies do not suffer from cooperative growth errors, they form an ideal system to demonstrate the idea of activated binding sites and serve as the first step in the demonstration of 2D activatable assemblies. We demonstrate the formation of two different 1-D DNA nanoassemblies using activatable tiles. Our first assembly is formed from tiles that are activated simultaneously, while our second assembly is formed from tiles that activate sequentially.

1-D Activatable Assemblies. *Mechanism 1: Simulatenous Activation of Tiles.* In this tile assembly, all the tiles are initially protected *via* protector strands (blue colored strands in Figures 2 and 3). These protector strands inhibit tiles from self-assembling to form the desired final assembly. On introduction of an initiator, the protector strands are removed *simultaneously*, resulting in the activation of the tiles, and subsequent assembly formation.

Mechanism 2: Directed Activation of Tiles. Similar to the previous mechanism, all the tiles are initially protected *via* protector strands. On the addition of an initiator, an initial set of protected seed tiles are activated. These active tiles can now attach to other protected tiles. Each protected tile that is attached subsequently gets deprotected (activated). Note that in case an incorrect tile is added to the growing assembly, that growth front of the assembly halts and the assembly does not grow until the incorrect tile detaches and the correct tile diffuses into the correct position.

Comparison of Mechanisms. Mechanism 1 is an example of *free self-assembly*, while Mechanism 2 is an example of *serial self-assembly*.[30] *Serial self-assembly* is expected to have lower nucleation errors, since it can

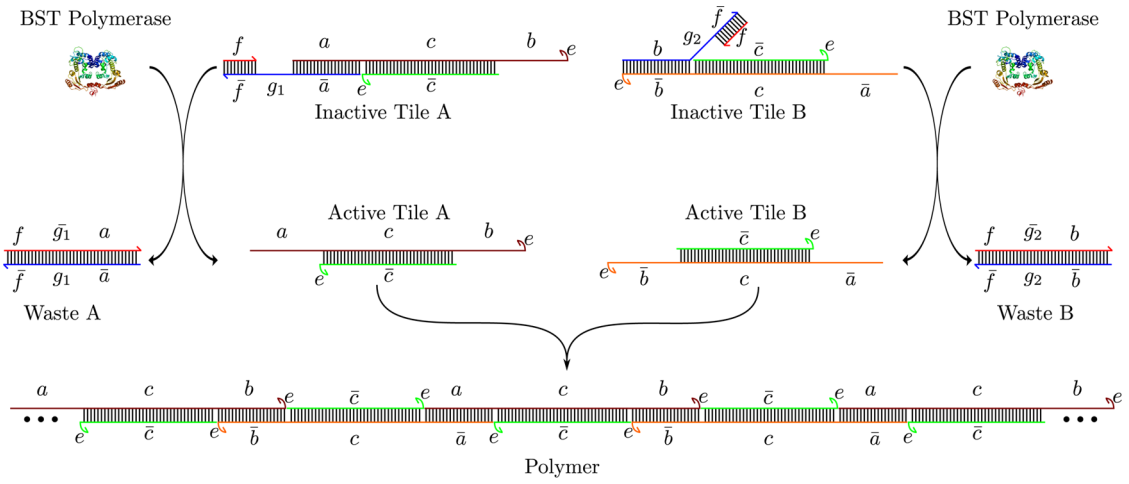

Figure 3. Co-polymerization of *Tile A* and *Tile B* after activation: figure shows two complexes, Inactive *Tile A* is composed of four strands: $\bar{c}e$, $\bar{a}g_1\bar{f}$, *acbe* and *f*. Inactive *Tile B* is composed of 4 strands: $\bar{c}e$, $bg_2\bar{f}$, $\bar{a}\bar{c}be$ and *f*. *BST* DNA Polymerase Large Fragment is illustrated by a protein cartoon and does not represent the actual tertiary structure of the enzyme. This strand displacing polymerase extends the primer strand *f* on both tiles exposing sticky ends *a* and $\bar{b}$ in tiles A and B, respectively. This transformation of Inactive *Tile A* and Inactive *Tile B* into Active *Tile A* and Active *Tile B* creates waste products Waste A and Waste B, respectively. Active *Tile A* and Active *Tile B* now co-polymerize into a long linear polymer.

initiate only from a seed. *Free self-assembly*, on the other hand, is driven by the spontaneous nucleation of tiles that takes place when tiles randomly moving around collide into one another. Systems that spontaneously nucleate lose entropy with every tile attachment, resulting in a low average tile-number per assembly. To form assemblies with a larger average number of tiles, we have to bias the reaction toward overcoming the entropic loss caused by the additional tiles being added to the assembly. This biasing can be done in two ways, by increasing the length of the sticky ends, or by using enzymatic methods that use an external energy source(s) (dNTPs).

Enzyme-Free Activated Tiles: Prior Protected and Layered Tile Mechanisms. Enzyme-free protocols have been suggested by Murata[44] and Fujibayashi *et al.*:[45,46] the Protected Tile Mechanism (PTM) and the Layered Tile Mechanism (LTM), which utilize DNA protecting molecules to form kinetic barriers against spurious assembly. Experimental work using these protocols has been demonstrated.[47] In particular, the authors introduce a protection strand covering the input sticky ends of DNA tiles, and this protection strand is removed only if both inputs correctly match. In the PTM, the output sticky ends are not protected and can bind to a growing assembly before the inputs are deprotected causing an error. In the LTM, the output sticky ends are protected only by 3 nucleotides each and can be easily displaced causing the above-mentioned error. Thus, only if we can ensure a deprotection from input to output end can error resilience be guaranteed. Our activatable tiles technique is a modest step toward this goal.

Design of Activatable Tiling Systems. *Mechanism 1: Simultaneous Activation of Tiles.* This section describes a prototype experiment to verify the activity of DNA polymerase on a tile system. We demonstrate a 1-D assembly formed from tiles that are all simultaneously activated. Note that this model is not an exact solution to the idea proposed in Majumder *et al.*,[43] since the tiles should instead be activated sequentially. This serves as a precursor to our experiments in the next section.

The initial configuration of the system consists of two tile types, both inactive. On the addition of *BST Polymerase*, all instances of both tile types become active, resulting in subsequent assembly formation. This experiment serves as a proof of concept, demonstrating that polymerase can be used as an initiator to activate a set of tiles.

The system consists of two tiles, *Tile A* and *Tile B*, each having two sticky ends (pads). Sticky ends are programmed such that the ends of *Tile A* can hybridize to the two sticky ends of *Tile B*. This results in a linear co-polymer of alternating *Tile A* and *Tile B*. The tiles themselves are DNA duplexes with overhangs that act as sticky ends. The sticky ends of each tile can be protected *via* hybridization with a protector complex rendering the tiles inactive. The protector complex contains a primer that can be extended by a strand displacing polymerase which results in deprotection of the tile. This system is illustrated in Figure 3.

The protected versions of *Tile A* and *B*, labeled *Inactive Tile A* and *Inactive Tile B*, are synthesized *via* annealing. *Inactive Tile A* is composed of two parts, *Active Tile A* and *Protector Complex A*. *Active Tile A*, composed of the strands *acbe* and $\bar{c}e$, is a dsDNA with overhangs. *Protector Complex A* consists of the strand $\bar{a}g_1\bar{f}$ and the primer *f*. Similarly, *Inactive Tile B* is composed of two parts, *Active Tile B* (composed of the strands $\bar{a}\bar{c}be$ and $\bar{c}e$) and *Protector Complex B* ($bg_2\bar{f}$ and the *Primer f*). *Inactive Tile A* and *Inactive Tile B* do not react with each other in solution.

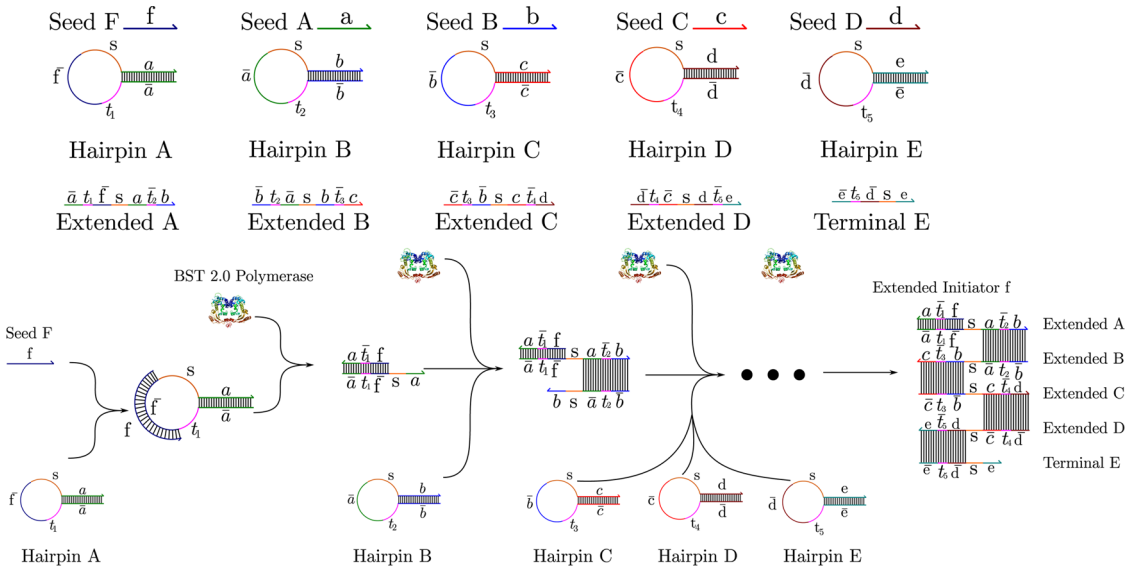

Figure 4. Directed assembly of tiles.

In the presence of the strand displacing *BST DNA Polymerase*, the primers on both the inactive tiles are extended to form waste products *Waste A* and *Waste B*. In doing so, the sticky end *a* of *Inactive Tile A* and sticky end $\overline{b}$ of *Inactive Tile B* are exposed. This activation event results in the formation of *Active Tile A* and *Active Tile B*, and they co-polymerize into a linear polymer with alternating A and B tiles. The 3′ ends of the four DNA strands composing the tiles are augmented with a special domain *e*, 3 nt (TTT), that is designed to have minimum interaction with any strand in the system. This unhybridized overhang ensures that the polymerase does not spuriously extend these strands.

An additional tile was synthesized by omitting one of the sticky ends in *Tile B*. Specifically, the sticky end $\overline{b}$ of the *Active Tile B* is omitted and this modified tile is labeled *Blunt Tile B*. *Active Tile A*, formed by the activation event described earlier, reacts with *Blunt Tile B* to form a dimer. This process is illustrated in Figure 2, and it serves as an additional experiment demonstrating the formation of a nanoassembly.

Mechanism 2: Directed Activation of Tiles. The scheme depicted in this section activates a tile on binding of the correct input tile (Figure 4). This is in contrast to the one-time switch mechanism of the previous section. Here, an incorrect binding causes the assembly to halt, since the next tile is not activated. The assembly begins with the addition of an initiator (analogous to a *seed tile* in the abstract Tile Assembly Model (aTAM),[42]) that only activates those **instances** of the tiles that have bound to the initiator. These tiles activate subsequent tiles, and the assembly grows at a rate proportional to the reactant concentration.

The system consists of five hairpins, named after their stem domains: *Tiles A*, *B*, *C*, *D*, and *E*. Each hairpin has a stem length of 21 nt (chosen to avoid opening of the hairpin at room temperature (RT)), and an unhybridized loop of 42 nt. The stem domains (dsDNA) are initially inactive. Note that overhangs in the hairpins are not needed, serendipitously removing a common source of leaks.

On addition of the initiator *Seed F*, *Tile A* is activated in the following manner: *Seed F* binds to the hairpin loop of *Tile A*, and the polymerase extends the strand, unravelling the stem domain *a*. Domain *a*, now single stranded, is free to bind to *Tile B*.

The addition of the initiator activates *Tile A*, which can now bind to *Tile B*. *Tile B* in turn activates *Tile C*, *Tile C* activates *Tile D*, and *Tile D* activates *Tile E*. The expected end product is shown in Figure 4. This duplex DNA nanostructure is of the form of a DNA ribbon. It has a central seam, which is the ssDNA section of the nanostructure, consisting of spacers. There are dsDNA helices on either end of 48 bp length.

RESULTS AND DISCUSSION

Simultaneous Activation Mechanism. Leaks in the absence of *BST Polymerase* were seen in both the dimer and polymer mechanisms. The polymer system showed a leak of 14.72% (lane 12, Figure 5, left), while the dimer system showed a leak of 11.5% (lane 8, Figure 5, right), calculations in Supporting Information Section S3.1. In other words, for every 100 tiles of *Inactive Tile A* and *Inactive Tile B*, approximately 15 tiles of *Inactive Tile A* and *Inactive Tile B* leaked to form a polymer over 3 h. (Similarly 12 tiles of *Inactive Tile A* and *Blunt Tile B* leaked to form a dimer.) We attribute this high error rate to the following reasons: (1) Stoichiometry imbalance in formation of tiles—malformed tiles and some tiles without the protector strand can contribute to the leak products observed. This could be fixed by further purification of the tiles postannealing. (2) There might be a low rate of dissociation at RT of the protector strands ($\overline{a}g_1\overline{f}$ and $bg_2\overline{f}$) that are bound

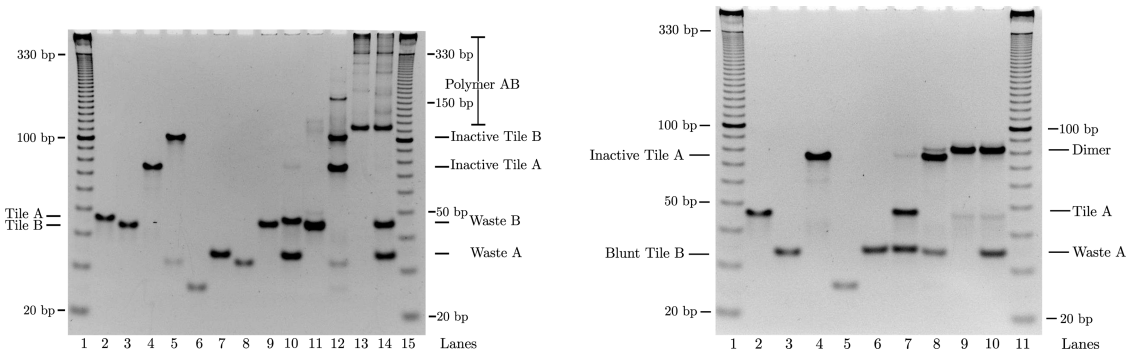

Figure 5. Formation of dimer and polymers. (Left) Polymerization of activatable tiles. Lanes 1 and 15, 10 bp ladder; lane 2, Active Tile A; lane 3, Active Tile B; lane 4, Inactive Tile A; lane 5, Inactive Tile B; lane 6, Primer + Protector A; lane 7, Primer + Protector A + BST; lane 8, Primer + Protector B; lane 9, Primer + Protector B + BST; lane 10, Inactive Tile A + BST; lane 11, Inactive Tile B + BST; lane 12, Inactive Tile A + Inactive Tile B; lane 13, Active Tile A + Active Tile B; lane 14, Inactive Tile A + Inactive Tile B + BST. (Right) Dimer formation. Lanes 1 and 11, 10 bp ladder; lane 2, Active Tile A, lane 3, Blunt Tile B; lane 4, Inactive Tile A; lane 5, Primer + Protector A; lane 6, Primer + Protector A + BST; lane 7, Inactive Tile A + BST; lane 8, Inactive Tile A + Blunt Tile B; lane 9, Active Tile A + Blunt Tile B; lane 10, Inactive Tile A + Blunt Tile B + BST.

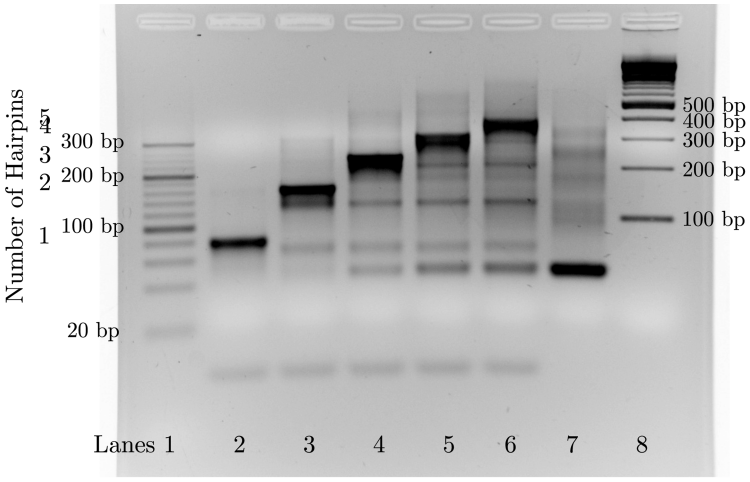

Lane	Yield
2	33.33%
3	27.33%
4	31.33%
5	19.33%
6	16%
7 (leak)	4%

Figure 6. Sequential assembly using BST 2.0 Polymerase at 52 °C. Lane 1, 20 bp ladder; lane 2, Hairpin A + Seed F (0.5 μM); lane 3, Hairpins A + B + Seed F (0.5 μM); lane 4, Hairpins A + B + C + Seed F (0.5 μM); lane 5, Hairpins A + B + C + D + Seed F (0.5 μM), lane 6, Hairpins A + B + C + D + E + Seed F (0.5 μM); lane 7, (Leak) Hairpins A + B + C + D + E (0.5 μM); lane 8, 2-log ladder.

by 16 nt. Increasing this length might help alleviate the leak rates.

Sequential Activation Mechanism. We have achieved directed linear assemblies of sizes 1−5 tiles. Experiments in the presence and absence of polymerase (Supporting Information Section S2.1.6) reveal leaks in the system. A leak is defined as the formation of the final tile relative to the quantity of the initial reactants in the absence of a certain initiator (either the polymerase or the seed). In the absence of polymerase (thus presence of initiator), there is no leak (Supporting Information Figure S9). This is expected, since there is no polymerase to extend the seed. However, leaks are seen in the presence of polymerase.

Quantitation of the gel fragments shows 45−60% yield for 1 hairpin complexes, ≈30−50% yield for 2−3 hairpin complexes, and ≈20−30% yield for 4−5 hairpin complexes. The leaks account for about 7% of the yield in 2 hairpin systems, 17−27% of the yield in 3 hairpin systems, 14−29% of the yield in 4 hairpin systems, and 25−30% of the yield in 5 hairpin systems. For Figure 6, the error rate is 15−18% per tile attachment. We attribute this high error rate to two reasons: (1) impurities in the synthesis of strands; (2) the error rate increases as the number of tiles increases, thus indicating factors such as steric hindrance that impede the growth of the assembly.

We hypothesize that this method can be scaled up to create larger assemblies. However, the rate of assembly growth might decrease with assembly size because of two reasons: (1) The primer is 21 nt long, and each of the arms of the tiles are 48 bp. For the primer to attach to another hairpin, it will need to be unprotected by the steric hindrances it faces from the other arms. Also, since the primer complement is present in the looped region of the hairpin, it is sterically unstable for the hairpin to move into a position favored by the primer to which to attach. (2) Not unlike the steric hindrance faced by the primer, it is also sterically unfavorable for the polymerase subunit

to attach to the 3′ end of the primer, and extend another copy of the hairpin, unless there is adequate room for the polymerase to attach (the size of the BST molecule (PDB ID: 1XWL) is ≈7.1 × 7.8 × 8.1 nm^3 [48] when visualized by Jmol.[49]). As the length of the assembly increases, the steric hindrances faced in the addition of a new hairpin, and in the involvement of the polymerase increase. We have reduced the steric hindrances by introducing "spacer" domains (denoted by domain *s*, poly-T of 15 nt), which will give room to the arms of the assembly to accommodate the polymerase and the hairpin motifs. Note the arms of the assembly are analogous to stiff rods, since their lengths lie within the persistence length of DNA. We hypothesize that larger spacer domains will allow scaling of the assembly to larger structures. Another consideration is sequence design; sequences having repeats of 1−4 nt should be avoided when using polymerase (Supporting Information Section S4).

Experiments with 0.1 units of polymerase show a significantly reduced yield for higher order hairpins (4 hairpins at 9.75% and 5 hairpins at 8.74% yields, Supporting Information Section S2.1.4), and marked streaking in the analytical gels. Thus, the quantity of the polymerase influences the expected yield. The use of *BST 2.0 Polymerase* in comparison to *BST Polymerase* also improves the yield of the system (Supporting Information Section S2.1.7).

Experiments at a lower concentration of 100 nM (Supporting Information Section S2.1.8) also resulted in assembly formation, though with a reduced rate. Control experiments with a hairpin missing revealed that the system works as expected, and halts whenever there is a break in the chain (Supporting Information Figure S5).

BST polymerase runs optimally at 65 °C, while its activity at 37 °C is reduced by at least a factor of 2 (Supporting Information Figure S8).[50] Since the T_m of these hairpins (70−75 °C) is substantially higher than that of a linear dsDNA of the same length,[51] we utilize the higher processivity of the enzyme, and increase the assembly yield by running the system at a higher temperature 52 °C.[52] The leaks were quantified as 6.04% at 50 °C, 3.98% at 52 °C and 6.45% at 54 °C, and thus, 52 °C was chosen as the default reaction temperature. However, a different temperature might result in better yields. With increasing temperature, the opening rate of a hairpin increases, leading to a higher chance of leak reactions. Increasing the stem length of the hairpins could reduce the opening rate of hairpins at high temperatures, and in turn, leaks. However, due to current limitations in the high error rate of synthesis of strands above 100 nt, our experiments are limited to oligos under 100 nt.

Extensions to 2-D and Other Applications. The 1-D sequential assembly system we have described above has a high error rate of 15−18% in comparison to other enzyme-free 1-D assembly systems with 2−5%[28] and 5−10%.[32] However, with large-scale improvements in the synthesis of (1) nucleic acid strands and (2) nucleic acid enzymes, we expect the error rates to decrease considerably.

The design we have proposed is currently irreversible. Thus, a tile cannot detach once it has attached to the next tile. However, reversibility is a prerequisite in a 2-D system, since an incorrect attachment is allowed to detach and reattach at another location. Future steps would include extending this work to 2-D, and they would require the introduction of reversibility into this system. Beyond their applications to computational tiling, activatable tiles can be used for building sensing[53] and concentration systems, and for reaction catalyzation.[43] The success achieved in engineering such assemblies point to the possibility of more complex activatable and computing systems[54] that can alleviate some of the errors encountered in tile-based DNA self-assembly. They also point to enzymatic methods of self-assembly in addition to the well-known non-enzymatic methods of assembling DNA nanostructures.

MATERIALS AND METHODS

Experiments: Simulatenous Activating Assemblies. This section provides details of the experimental setup and data obtained from the experiments. After the domain level design of the system, DNA sequences assigned to each domain were designed by hand, taking care to minimize sequence symmetry. The length of the protecting strand $bg_2\bar{f}$ was designed to be greater than the length of the protecting strand $\bar{a}g_1\bar{f}$ to clearly separate the two complexes in analytical gels. The sequences were validated for any spurious secondary structures *via* the aid of online DNA folding servers.[55,56] The optimized sequences were obtained at 100 nmol synthesis scale from IDT DNA with standard desalting. DNA strands were PAGE purified and brought up to a working stock concentration of 20 μM. The inactive tile complexes were formed by mixing the constituent strands at an equimolar ratio of 1 μM in 20 μL reaction volume, the only exception being the primer strand *f* which was added in 2× excess as lower primer concentrations resulted in decreased yield of inactive tiles. The mixture was then heated to 90 ° C in a buffer of 1× TAE with 12.5 mM Mg^{2+} ions and cooled to room temperature (RT ≈ 23 °C) over 3 h.

A total of 1600 units of *BST DNA Polymerase*, Large Fragment at concentration 8000 units/mL was ordered from New England Biolabs. To test the activatable system, 4 pmol each of Inactive *Tile A* and Inactive *Tile B* with 0.1 unit of *BST DNA Polymerase* was incubated in a reaction buffer of 1× Thermopol (20 mM Tris-HCl, 10 mM $(NH_4)_2SO_4$, 10 mM KCl, 2 mM $MgSO_4$ and 0.1% Triton X-100) with 100 μg/mL BSA and 200 μM each of dATP, dCTP, dGTP, and dTTP for 3 h at RT. As a positive control, *Active Tile A* and *Active Tile B* were prepared in separate tubes, subsequent to which 4 pmol each was added to 0.1 units of the polymerase and incubated at RT for 3 h (lane 13, Figure 5, left). Likewise, 4 pmol each of *Inactive Tile A* and *Inactive Tile B* was incubated in the polymerase reaction buffer in the absence of *BST DNA Polymerase* at RT for 3 h (negative control, lane 12, Figure 5, left). In another control experiment, 4 pmol each of the protector complex ($\bar{a}g_1\bar{f} + f$ and $bg_2\bar{f} + f$) was incubated in separate test tubes with *BST DNA Polymerase* in polymerase buffer at RT

for 3 h (lanes 7 and 9: Figure 5, left). The complexes were then analyzed in 10% Nondenaturing PAGE Gels. The gels and running buffer contain 1× TAE with 12.5 mM Mg^{2+}. The gels were run for 7 h at 125 V and then stained and destained using ethidium bromide for 45 min each. Images were obtained using an Alpha Innotech Alphalmager system.

Figure 5, left, is a nondenaturing PAGE gel image showing the results of these experiments. Lane 14 shows the working of the system where *Inactive Tile A* and *Inactive Tile B* are incubated in polymerase buffer with *BST DNA Polymerase*. We see that the tiles are activated leading to the formation of *Waste A* and *Waste B* and the activated tiles form a linear polymer. Figure 5, right, is a nondenaturing PAGE gel image showing the results of a similar experiment in the modified system with *Blunt Tile B* resulting in the formation of a dimer.

The experiment above could be performed enzyme-free, by replacing the polymerase with two activating strands $f\bar{g}_1a$ and $f\bar{g}_2\bar{b}$. However, the advantage of using polymerase is that its activity in conjunction with the primer is sequence independent. Hence, a single primer could perform the activation on *both* the strands, as opposed to a need for two distinct activation strands. Also, this could be scaled up to a system containing a larger number of tiles, with a single trigger for activation. The trigger could be the addition of polymerase, or the addition of a single primer insofar as all the protecting strands share the same primer(s).

Experiments: Directed Activating Assemblies. This system consists of five hairpins: A($\bar{a}t_1\bar{f}sa$), B($\bar{b}t_2\bar{a}sb$), C($\bar{c}t_3\bar{b}sc$), D($\bar{d}t_4\bar{c}sd$), and E($\bar{e}t_5\bar{d}se$), that are each 84 nt in length. The sequences Seeds F(*f*), A(*a*), B(*b*), C(*c*), D(*d*) each have a single domain 21 nt in length. These domains *f*, *a*, *b*, *c*, *d*, and *e* are primer domains that get activated sequentially. The domains t_1-t_5 are 6 nt, while the spacer domain *s* is a poly-T of 15 nt. These have been included to avoid steric hindrances on primer binding. The persistent length of dsDNA is approximately 50 nm, ≈150 bp,[57] and the role of the domains t_1-t_5 is to increase the size of the hairpin loop so that the binding of the primer to the loop does not result in molecular beacon like activity, initiating a leak reaction.

The hairpins were created in 5 μM aliquots, and were "quick-annealed", by heating to 90 °C (5 min) and cooled at RT (5 min). A total of 1600 units of *BST 2.0 DNA Polymerase* at concentration 8000 units/mL was ordered from New England Biolabs. Two microliters of each hairpin (10 pmol), 4 μL of the seed (20 pmol, at 2× concentration to ensure all reactions proceed to completion), and 2 units of *BST 2.0 DNA Polymerase* were incubated in a reaction buffer of 1× Isothermal Amplification Buffer (20 mM Tris-HCl, 10 mM $(NH_4)_2SO_4$, 50 mM KCl, 2 mM $MgSO_4$ and 0.1% Tween20) with 100 μg/mL BSA and 1 mM each of dATP, dCTP, dGTP, and dTTP for 1 h at 52 °C. The hairpins were mixed stoichiometrically to achieve a final concentration of 0.5 μM (Seed 1 μM) in a total reaction volume of 20 μL. Ten microliters of mineral oil (M5904 Sigma, density 0.84 g/mL) was added to the total reaction mixture preincubation, to prevent evaporation. Four microliters of 6× Native Dye (0.25% bromophenol blue, 0.25% xylene cyanol, 12.5 mM TAE/Mg^{2+}, 50% glycerol) was added postincubation, and 3.6 μL (1.5 pmol) of the complexes was analyzed in 3% native agarose gels (5 mm thick, 27 mL, prepared for use in LB Buffer (Faster Better Media, LLC)). The agarose gels were prerun empty for 2 min, and then run with samples for 20 min at 250 V (in an ice bath to prevent curved gel bands). Images were obtained using an Alpha Innotech Alphalmager system. The results of the experiments can be seen in Figure 6. Stepwise reactions have been performed to verify the activity of one, two, three, four, and five hairpins, each step involving a single seed and DNA polymerase (Supporting Information Section S2.1). Reactions are performed at 52 °C (and 37 °C; Supporting Information Section S2.1.5) lower than the T_m of each tile (70−75 °C). Negative control experiments involving only the hairpins (with/without polymerase and/or primer) reveal 0−20% leaks in the system. The leaks, however, vary with temperature (Supporting Information Section S2.1.4).

Conflict of Interest: The authors declare no competing financial interest.

Acknowledgment. The authors thank Tianqi Song, Hieu Bui, Reem Mokhtar and the anonymous reviewers, for their valuable suggestions and critiques on the article. This work was supported in part by NSF CCF-1217457, NSF CCF-1141847 and NSF EMT Grant CCF-0829798.

Supporting Information Available: DNA sequence design and control experiments. This material is available free of charge *via* the Internet at http://pubs.acs.org.

REFERENCES AND NOTES

1. Winfree, E.; Liu, F.; Wenzler, L.; Seeman, N. Design and Self-Assembly of Two-Dimensional DNA Crystals. *Nature* **1998**, *394*, 539–544.
2. LaBean, T.; Yan, H.; Kopatsch, J.; Liu, F.; Winfree, E.; Reif, J.; Seeman, N. Construction, Analysis, Ligation, and Self-Assembly of DNA Triple Crossover Complexes. *J. Am. Chem. Soc.* **2000**, *122*, 1848–1860.
3. Yan, H.; Park, S. H.; Finkelstein, G.; Reif, J.; LaBean, T. DNA-Templated Self-Assembly of Protein Arrays and Highly Conductive Nanowires. *Science* **2003**, *301*, 1882–1884.
4. Shih, W.; Quispe, J.; Joyce, G. A 1.7-kilobase Single-Stranded DNA that Folds into a Nanoscale Octahedron. *Nature* **2004**, *427*, 618–621.
5. He, Y.; Chen, Y.; Liu, H.; Ribbe, A.; Mao, C. Self-Assembly of Hexagonal DNA Two-Dimensional (2D) Arrays. *J. Am. Chem. Soc.* **2005**, *127*, 12202–12203.
6. Rothemund, P. Folding DNA to Create Nanoscale Shapes and Patterns. *Nature* **2006**, *440*, 297–302.
7. He, Y.; Ye, T.; Su, M.; Zhang, C.; Ribbe, A.; Jiang, W.; Mao, C. Hierarchical Self-Assembly of DNA into Symmetric Supramolecular Polyhedra. *Nature* **2008**, *452*, 198–201.
8. Douglas, S.; Dietz, H.; Liedl, T.; Hogberg, B.; Graf, F.; Shih, W. Self-Assembly of DNA into Nanoscale Three-Dimensional Shapes. *Nature* **2009**, *459*, 414–418.
9. Dietz, H.; Douglas, S.; Shih, W. Folding DNA into Twisted and Curved Nanoscale Shapes. *Science* **2009**, *325*, 725–730.
10. Zheng, J.; Birktoft, J.; Chen, Y.; Wang, T.; Sha, R.; Constantinou, P.; Ginell, S.; Mao, C.; Seeman, N. From Molecular to Macroscopic *via* the Rational Design of a Self-Assembled 3D DNA Crystal. *Nature* **2009**, *461*, 74–78.
11. Yurke, B.; Turberfield, A.; Mills, A.; Simmel, F.; Neumann, J. A DNA-Fuelled Molecular Machine Made of DNA. *Nature* **2000**, *406*, 605–608.
12. Sherman, W.; Seeman, N. A Precisely Controlled DNA Biped Walking Device. *Nano Lett.* **2004**, *4*, 1203–1207.
13. Shin, J.-S.; Pierce, N. A Synthetic DNA Walker for Molecular Transport. *J. Am. Chem. Soc.* **2004**, *126*, 10834–10835.
14. Tian, Y.; Mao, C. Molecular Gears: A Pair of DNA Circles Continuously Rolls against Each Other. *J. Am. Chem. Soc.* **2004**, *126*, 11410–11411.
15. Yin, P.; Choi, H.; Calvert, C.; Pierce, N. Programming Biomolecular Self-Assembly Pathways. *Nature* **2008**, *451*, 318–322.
16. Green, S.; Bath, J.; Turberfield, A. Coordinated Chemomechanical Cycles: A Mechanism for Autonomous Molecular Motion. *Phys. Rev. Lett.* **2008**, *101*, 238101–238104.
17. Venkataraman, S.; Dirks, R.; Rothemund, P.; Winfree, E.; Pierce, N. An Autonomous Polymerization Motor Powered by DNA Hybridization. *Nat. Nanotechnol.* **2007**, *2*, 490–494.
18. Yin, P.; Yan, H.; Daniell, X.; Turberfield, A.; Reif, J. A Unidirectional DNA Walker Moving Autonomously along a Linear Track. *Angew. Chem., Int. Ed.* **2004**, *116*, 5014–5019.
19. Bath, J.; Green, S.; Turberfield, A. A Free-Running DNA Motor Powered by a Nicking Enzyme. *Angew. Chem., Int. Ed.* **2005**, *44*, 4358–4361.
20. Sahu, S.; LaBean, T.; Reif, J. A DNA Nanotransport Device Powered by Polymerase ϕ29. *Nano Lett.* **2008**, *8*, 3870–3878.
21. Park, S. H.; Pistol, C.; Ahn, S. J.; Reif, J.; Lebeck, A.; LaBean, C. D. T. Finite-Size, Fully Addressable DNA Tile Lattices Formed by Hierarchical Assembly Procedures. *Angew. Chem., Int. Ed.* **2006**, *45*, 735–739.

22. Rothemund, P.; Papadakis, N.; Winfree, E. Algorithmic Self-Assembly of DNA Sierpinski Triangles. *PLoS Biol.* **2004**, *2*, 424–436.
23. Rothemund, P.; Winfree, E. The Program-Size Complexity of Self-Assembled Squares. *Symp. Theor.Comput.* **2000**, 459–468.
24. Adleman, L. Molecular Computation of Solutions to Combinatorial Problems. *Science* **1994**, *266*, 1021–1024.
25. Winfree, E.; Yang, X.; Seeman, N. Universal Computation *via* Self-Assembly of DNA: Some Theory and Experiments. In *DNA Based Computers II: DIMACS Workshop, June 10-12, 1996* ; Landweber, L. F., Baum, E. B., Eds.; American Mathematical Society: Providence, RI, 1996; Vol. 44, pp 191−213.
26. Reif, J. Local Parallel Biomolecular Computation. In *DNA-Based Computers III: DIMACS Workshop, June 23-25, 1997*; Rubin, H., Wood, D. H., Eds.; American Mathematical Society: Providence, RI, 1997; pp 217−254.
27. Reif, J.; LaBean, T.; Sahu, S.; Yan, H.; Yin, P. In *Unconventional Programming Paradigms*; Bantre, J.-P., Fradet, P., Giavitto, J.-L., Michel, O., Eds.; Lecture Notes in Computer Science; Springer: Berlin Heidelberg, 2005; Vol. 3566; pp 173−187.
28. Mao, C.; Labean, T.; Reif, J.; Seeman, N. Logical Computation Using Algorithmic Self-Assembly of DNA Triple-Crossover Molecules. *Nature* **2000**, *407*, 493–496.
29. Winfree, E.; Eng, T.; Rozenberg, G. String Tile Models for DNA Computing by Self-Assembly. *DNA Comput.* **2000**, 63–88.
30. LaBean, T.; Winfree, E.; Reif, J. Experimental Progress in Computation by Self-Assembly of DNA Tilings. In *DNA Based Computers V, DIMACS*; Winfree, E., Gifford, D. K., Eds.; American Mathematical Society, 2000; Vol. 54, pp 123−140.
31. Chandran, H.; Gopalkrishnan, N.; Reif, J. The Tile Complexity of Linear Assemblies; *International Colloquium on Automata, Languages and Programming*; Springer: Berlin, 2009; pp 235−253.
32. Schulman, R.; Lee, S.; Papadakis, N.; Winfree, E. One Dimensional Boundaries for DNA Tile Self-Assembly. *DNA Comput.* **2003**, 108–126.
33. Demaine, E.; Eisenstat, S.; Ishaque, M.; Winslow, A. In *DNA Computing and Molecular Programming*; Cardelli, L., Shih, W., Eds.; Lecture Notes in Computer Science; Springer: Berlin, Heidelberg, 2011; Vol. 6937; pp 100−114.
34. Fujibayashi, K.; Hariadi, R.; Park, S. H.; Winfree, E.; Murata, S. Toward Reliable Algorithmic Self-Assembly of DNA Tiles: A Fixed-Width Cellular Automaton Pattern. *Nano Lett.* **2008**, *8*, 1791–1797.
35. Barish, R. D.; Schulman, R.; Rothemund, P. W. K.; Winfree, E. An Information-Bearing Seed for Nucleating Algorithmic Self-Assembly. *Proc. Natl. Acad. Sci. U.S.A.* **2009**, *106*, 6054–6059.
36. Chen, H.-L.; Doty, D. Parallelism and Time in Hierarchical Self-assembly; *Proceedings of the Twenty-third Annual ACM-SIAM Symposium on Discrete Algorithms*; SIAM: Philadelphia, PA, 2012; pp 1163−1182.
37. Schulman, R.; Yurke, B.; Winfree, E. Robust Self-Replication of Combinatorial Information *via* Crystal Growth and Scission. *Proc. Natl. Acad. Sci. U.S.A.* **2012**, *109*, 6405–6410.
38. Winfree, E.; Bekbolatov, R. Proofreading Tile Sets: Error Correction for Algorithmic Self-Assembly. *DNA Comput.* **2003**, 126–144.
39. Chen, H.-L.; Goel, A. Error Free Self-assembly Using Error Prone Tiles. *DNA Comput.* **2004**, 62–75.
40. Reif, J.; Sahu, S.; Yin, P. Compact Error-Resilient Computational DNA Tiling Assemblies. *DNA Comput.* **2004**, 293–307.
41. Rothemund, P. W. K. Using Lateral Capillary Forces to Compute by Self-Assembly. *Proc. Natl. Acad. Sci. U.S.A.* **2000**, *97*, 984–989.
42. Winfree, E. Algorithmic Self-Assembly of DNA. Ph.D. Thesis, California Institute of Technology, 1998.
43. Majumder, U.; LaBean, T.; Reif, J. In *DNA Comput.*; Garzon, M., Yan, H., Eds.; Lecture Notes in Computer Science; Springer: Berlin, Heidelberg, 2008; Vol. 4848; pp 15−25.
44. Murata, S. Self-Assembling DNA Tiles—Mechanisms of Error Suppression. *SICE 2004 Annual Conference*; IEEE: Piscataway, NJ, **2004**; Vol. *3*, pp 2764−2767
45. Fujibayashi, K.; Murata, S. A Method of Error Suppression for Self-Assembling DNA Tiles. *DNA Comput.* **2005**, *3384*, 113–127.
46. Fujibayashi, K.; Zhang, D. Y.; Winfree, E.; Murata, S. Error Suppression Mechanisms for DNA Tile Self-Assembly and Their Simulation. *Nat. Comput.* **2009**, *8*, 589–612.
47. Zhang, D. Y.; Hariadi, R. F.; Choi, H. M.; Winfree, E. Integrating DNA Strand-Displacement Circuitry with DNA Tile Self-Assembly. *Nat. Commun.* **2013**, *4*, 1965.
48. Kiefer, J. R.; Mao, C.; Hansen, C. J.; Basehore, S. L.; Hogrefe, H. H.; Braman, J. C.; Beese, L. S. Crystal Structure of a Thermostable Bacillus DNA Polymerase I Large Fragment at 2.1 Resolution. *Structure* **1997**, *5*, 95–108.
49. Hanson, R. M.; Prilusky, J.; Renjian, Z.; Nakane, T.; Sussman, J. L. JSmol and the Next-Generation Web-Based Representation of 3D Molecular Structure as Applied to Proteopedia. *Isr. J. Chem.* **2013**, *53*, 207–216.
50. Stenesh, J.; Roe, B. DNA Polymerase from Mesophilic and Thermophilic Bacteria: I. Purification and Properties of DNA Polymerase from Bacillus Licheniformis and Bacillus Stearothermophilus. *Biochim. Biophys. Acta, Nucleic Acids Protein Synth.* **1972**, *272*, 156–166.
51. Paner, T. M.; Amaratunga, M.; Doktycz, M. J.; Benight, A. S. Analysis of Melting Transitions of the DNA Hairpins Formed from the Oligomer Sequences d[GGATAC-(X)4GTATCC] (X = A, T, G, C). *Biopolymers* **1990**, *29*, 1715–1734.
52. Notomi, T.; Okayama, H.; Masubuchi, H.; Yonekawa, T.; Watanabe, K.; Amino, N.; Hase, T. Loop-Mediated Isothermal Amplification of DNA. *Nucleic Acids Res.* **2000**, *28*, e63.
53. Chandran, H.; Rangnekar, A.; Shetty, G.; Schultes, E. A.; Reif, J. H.; LaBean, T. H. An Autonomously Self-Assembling Dendritic DNA Nanostructure for Target DNA Detection. *Biotechnol. J.* **2013**, *8*, 221–227.
54. Chandran, H.; Garg, S.; Gopalkrishnan, N.; Reif, J. *Biomolecular Information Processing: From Logic Systems to Smart Sensors and Actuators*; Wiley-VCH Verlag GmbH & Co. KGaA: Weinheim, 2012; pp 199−220.
55. Zuker, M. MFOLD Web Server for Nucleic Acid Folding and Hybridization Prediction. *Nucleic Acids Res.* **2003**, *31*, 3406–3415.
56. Zadeh, J.; Steenberg, C.; Bois, J.; Wolfe, B.; Pierce, M.; Khan, A.; Dirks, R.; Pierce, N. NUPACK: Analysis and Design of Nucleic Acid Systems. *J. Comput. Chem.* **2010**, *32*, 170–173.
57. Hays, J. B.; Magar, M. E.; Zimm, B. H. Persistence Length of DNA. *Biopolymers* **1969**, *8*, 531–536.